# GFD 2017 Lecture 2: Ice Dynamics

Andrew Fowler; notes by Federico Fuentes and Madelaine Gamble Rosevear

June 20, 2017

This document comprises the first full lecture given by Andrew Fowler during the 2017 Geophysical Fluid Dynamics program at the Woods Hole Oceanographic Institution (WHOI). It is about ice dynamics, and is divided in two parts: ice sheet flow, and sliding and subglacial hydrology. Most of the details were taken from Dr. Fowler's book [Fowler, 2011], which the reader is invited to consult if more information is required.

## 1 Ice sheet flow

### 1.1 Governing equations

Over sufficiently long periods, ice behaves as a viscous fluid, deforming under applied stress. The strain rate $\dot{\varepsilon}_{ij}$ is given by

$$\dot{\varepsilon}_{ij} = \frac{1}{2}\left(\frac{\partial u_i}{\partial x_j} + \frac{\partial u_j}{\partial x_j i}\right), \tag{1}$$

and is commonly modeled using Glen's flow law

$$\dot{\varepsilon}_{ij} = A(T)\tau^{n-1}\tau_{ij}\,, \tag{2}$$

where $\tau_{ij}$ is the deviatoric stress tensor in index notation, $\tau$ is the second stress invariant, defined by $2\tau^2 = \tau_{ij}\tau_{ij}$, and $A(T)$ is a temperature dependent term. The Glen exponent $n$ is typically taken to be 3, although values $1 \leq n \leq 4$ have been proposed in the literature.

For the flow of a glacier the Reynolds number is approximately $10^{-13}$, so inertial terms are small with respect to viscous terms (Stokes flow) and mass and momentum conservation may be expressed as

$$\boldsymbol{\nabla \cdot u} = 0 \tag{3}$$

$$0 = \boldsymbol{\nabla} p + \boldsymbol{\nabla \cdot \tau} + \rho \boldsymbol{g}. \tag{4}$$

where $p$ is the pressure, $\boldsymbol{g}$ is the gravity vector and $\boldsymbol{\tau}$ is the deviatoric part of the stress tensor. The assumption of incompressibility in (3) holds within the ice. This is a reasonable assumption as the surface layer in which snow and firn are compacted into ice is very thin.

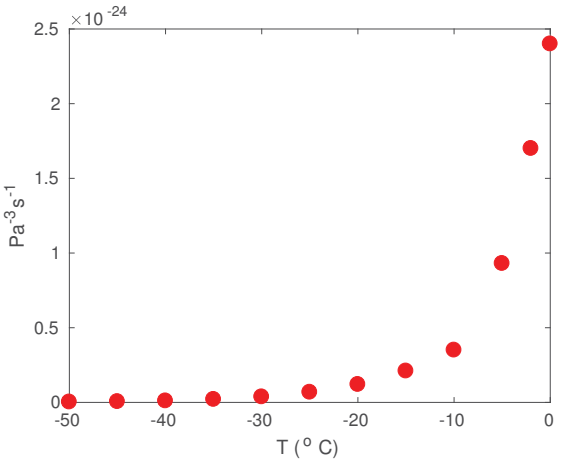


Figure 1: Controls on Creep Parameter A. Data from [Cuffey and Paterson, 2010].

Finally we have the energy equation:

$$\rho c_p(T_t + \underbrace{\boldsymbol{u}\cdot\boldsymbol{\nabla}T}_{\text{advection}}) = \underbrace{k\nabla^2 T}_{\substack{\text{heat}\\ \text{conduction}}} + \underbrace{\tau_{ij}\dot{\varepsilon}_{ij}}_{\substack{\text{viscous}\\ \text{dissipation}}} \tag{5}$$

where $\rho$ is the ice density, $c_p$ is the specific heat, and $k$ is the thermal conductivity. The final term in (5) is the viscous heating term describing the conversion of mechanical energy to heat. Whilst this term is often neglected in other geophysical flows, it significant for ice sheet flow.

Stress and strain are related by $\tau_{ij} = 2\eta\dot{\varepsilon}_{ij}$ where $\eta$ is the effective viscosity. Using (2) we can write

$$\eta = \frac{1}{2A(T)\tau^{n-1}}. \tag{6}$$

The term $A(T)$ is strongly dependent on temperature, increasing over three orders of magnitude for a temperature change of 50 K (Figure 1), and thus viscosity is inversely related to temperature.

### 1.2 Bi-stability and thermal runaway

It is the strong temperature dependence of the viscous heating term that provides the mechanism for "thermal runaway". If heat is supplied to the ice, the temperature increases and the viscosity decreases. This allows the ice to flow faster, increasing stresses at the bed and warming the ice through the viscous heating term in (5). This in turn lowers viscosity, creating a positive feedback loop.

### 1.3 Boundary conditions

A complicating factor for the modeling of ice flows is that one cannot assume a no-slip boundary condition at the bedrock. Water present beneath the ice allows sliding, and thus

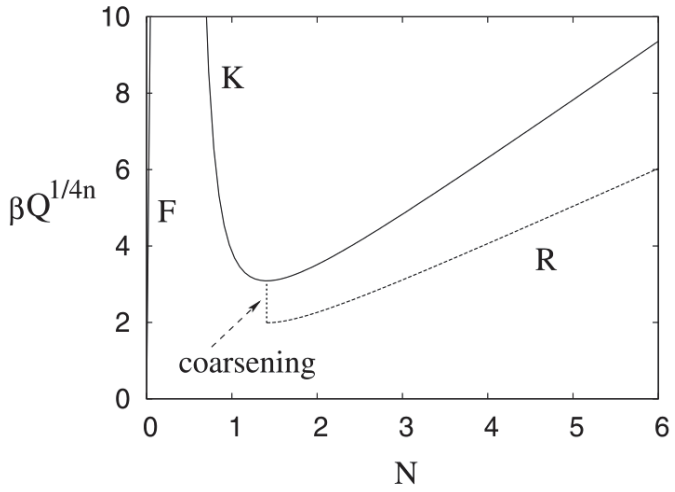


Figure 2: Illustrative relation between the effective pressure $N$ and the water flow $Q$ through a field of linked cavities [Fowler, 2011] where $F$ represents film flow, $K$ is linked cavities and $R$ is Röthlisberger channels. To the right of the minimum, distributed drainage is unstable; the channels coarsen resulting in a single Röthlisberger channel. To the left, distributed drainage in the form of linked cavities is stable. As $N$ goes to zero a thin film flow is permitted.

a sliding law is required. The basal stress,

$$\tau_b = N f\left(\frac{u_b}{N^n}\right) , \tag{7}$$

is modeled as an increasing function $f$ of the velocity at the base $u_b$ and the effective pressure $N = p_i - p_w$, where $p_i$ is the overburden pressure and $p_w$ is the water pressure. The effective pressure, $N$, is analogous to that used in soil mechanics, and is typically positive. In order to relate $N$ to the subglacial water flow rate $Q$, subglacial hydraulic theory is required. Three of the prevailing theories, are:

- Röthlisberger channels, where
$$N \approx \beta Q^{1/(4n)} . \tag{8}$$

- A linked system of canals, where
$$N \approx \frac{\gamma}{Q^{1/n}} . \tag{9}$$

- A Creyts-Schoof film, where
$$N \approx \frac{\delta}{Q^{\mu}} . \tag{10}$$

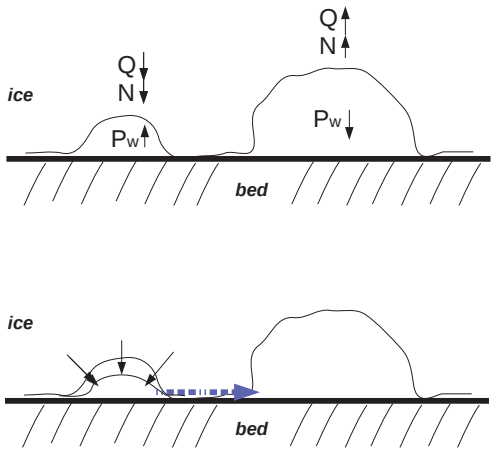


Figure 3: Schematic showing the draining and subsequent closure of a smaller channel due to the presence of a neighboring larger channel.

### 1.3.1 Röthlisberger channels

Subglacial water is present due to both basal melt and, where a conduit to the base is present, surface melt or rainfall. One theory of subglacial drainage involves the formation of semi-circular channels within the ice. The fact that the effective pressure $N$ is typically positive means that these channels would close through the deformation of the ice in the absence of a mechanism to keep them open. This mechanism is melting due to frictional heating from the water flow.

The expression for the effective pressure of one of these channels is

$$N \sim \beta Q^{1/4n} \tag{11}$$

where $Q$ is the flow rate of the water and $\beta$ is a material parameter that depends inversely on roughness.

An interesting feature of this system is that a decrease in water flux decreases $N$ and therefore *increases* the water pressure $p_w$. If we consider a small channel next to a large channel (Figure 3), then $Q$ is small within the small channel, and thus the water pressure $p_w$ must be large. In the larger channel the opposite is true, so the water pressure is low. The bed separating the two is rough, and water is able to leak from high to low pressure. As a result of this, smaller channels drain towards larger ones and close down, creating an arterial system of channels.

## 1.4 Thermal boundary conditions

The pressure melting point of ice decreases with increasing pressure, meaning that even very cold ice may be above the *in-situ* melting temperature at the base of an ice sheet. This

means we need to consider whether the ice is above or below the melting point in our thermal boundary conditions. When the temperature at $z = b$ is less than the freezing temperature $T_m$ the ice is frozen to the bed and we have a no slip boundary,

$$-k\frac{\partial T}{\partial n} = G\,, \quad T < T_m\,, \quad u = 0\,, \tag{12}$$

where $G$ is the geothermal heat flux and $n$ is direction normal to the bed. Once the base reaches the melting temperature a layer of water is present, lubricating the base of the ice. This allows some sliding, however less than the full sliding velocity $u_b$ as there is not yet a net production of water,

$$-k\frac{\partial T}{\partial n} = G + \tau_b u\,, \quad T = T_m\,, \quad 0 < u < u_b\,. \tag{13}$$

This introduces a frictional heating term $\tau_b u$ due to the sliding. When there is net production of water, the ice attains its full sliding velocity. In this regime,

$$0 < -k\frac{\partial T}{\partial n} < G + \tau_b u\,, \quad T = T_m\,, \quad u = u_b\,. \tag{14}$$

Note that each of these regimes contains an inequality, adding another layer of complexity to the model.

### 1.5 Shallow ice approximation

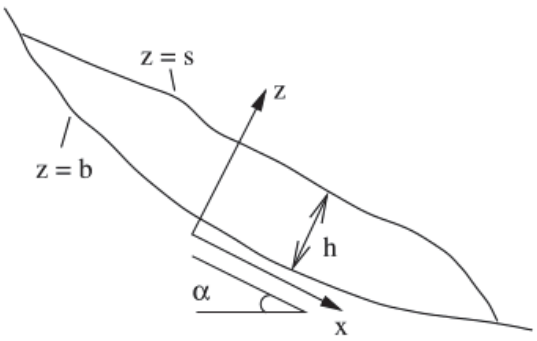


Figure 4: Schematic of a valley glacier showing thickness $h$ (elsewhere $H$), bed elevation $b$ and surface height $s$. Figure from [Fowler, 2011].

Ice sheets may be thousands of kilometers in extent but are only kilometers deep (Figure 5), allowing the use of the shallow ice approximation. For an ice sheet of thickness $d$ and extent $l$ the aspect ratio is given by $\varepsilon = d/l$. For the Antarctic Ice Sheet $d \sim 3 \times 10^3$ m, $l \sim 3 \times 10^6$ m giving $\varepsilon \sim 10^{-3}$. As a result of this, longitudinal derivatives of stress, velocity and temperature are small compared to vertical derivatives and may be neglected, reducing

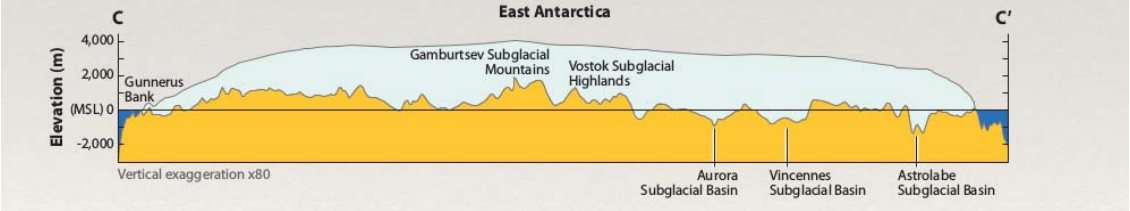


Figure 5: Cross section of the Antarctic Ice Sheet with exaggerated vertical scale. Figure from lecture slides.

the problem to a balance between the driving stress due to surface slope and resistive forces at the boundaries [Huybrechts, 2007].

This allows us to write a diffusion equation governing the evolution of the ice sheet thickness, $H$,

$$H_t = \boldsymbol{\nabla} \cdot \left( \underbrace{\left( \frac{|\boldsymbol{\nabla} s|^{n-1} H^{n+2}}{n+2} \boldsymbol{\nabla} s \right)}_{\text{nonlinear diffusion}} - H \boldsymbol{u}_b \right) + a \,, \tag{15}$$

where $H$ is the thickness of the ice sheet, $b$ is the bed elevation, $\boldsymbol{u}_b$ is the basal velocity, $s = H + b$ is the surface elevation and $a$ is the accumulation from snowfall (or, where negative, ablation). The nonlinear diffusion causes degeneracy at the boundaries and singularities may be involved. Whilst the term $-H\boldsymbol{u}_b$ looks like an advective term, $\boldsymbol{u}_b$ is typically in the direction of the shear stress and so is proportional to the surface slope ($\boldsymbol{u}_b \sim \tau_b \sim -\boldsymbol{\nabla} s$), meaning that this term is also diffusive.

### 1.6 Accumulation and hysteresis

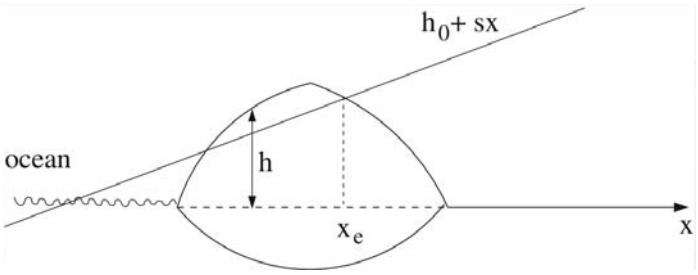


Figure 6: Schematic of an ice sheet with extent $x_e$ and height $H$.

Ice sheet mass is determined by the balance between accumulation of snow above the snow line and ablation at the margins, where the snow line is given by $h_0 + sx$, as shown in Figure 6. As the ice sheet extent decreases the height $h$ decreases, meaning less of the ice sheet is above the snow line, and therefore accumulation is less and ice sheet extent decreases. When the height falls beneath the snow line accumulation goes to zero. In the absence of any gain terms, the ice sheet collapses.

## 2 Sliding and Subglacial Hydrology

### 2.1 Weertman's sliding law

Consider ice over a set of obstacles as illustrated in Figure 7. The obstacles are separated on average by a distance $l$ and have heights roughly of size $a$, so that the aspect ratio is defined as

$$\nu = \frac{a}{l}\,. \tag{16}$$

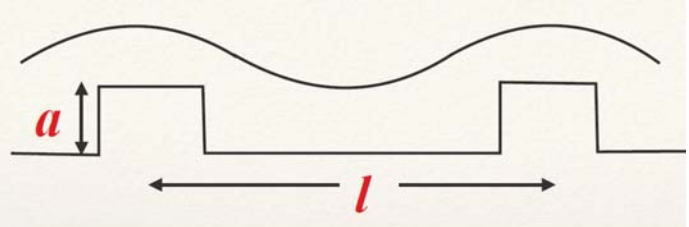


Figure 7: Weertman's sliding law.

The ice is assumed to slide at a particular velocity. Weertman's law is derived by assuming that a "regelation" velocity is roughly the same as a "viscous" velocity associated to Glen's flow law.

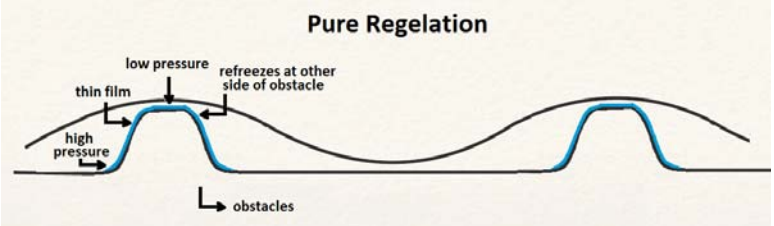


Figure 8: Pure regelation.

Regelation occurs when ice at high pressure melts and then refreezes at areas of low pressure. This creates a very thin film, with a thickness of the order of $1\mu$m over which the ice flows. Figure 8 shows the case of pure regelation. Under regelation, the pressure difference across the obstacle is roughly

$$\delta p \approx -\frac{\tau}{\nu^2}\,, \tag{17}$$

where $\tau$ is the average shear stress at the bed, and $p$ is the pressure. Hence, using that

$$-\frac{dT_m}{dp} = C\,, \tag{18}$$

where $T_m$ is the melting temperature, it follows that there is a temperature difference of

$$\delta T \approx C\frac{\tau}{\nu^2}\,, \tag{19}$$

where $T$ is the temperature. The regelative water flux is $u_R a^2$, where $u_R$ is the regelative ice velocity, meaning that to melt the ice a latent heat of $\rho_i L u_R a^2$ is necessary, where $\rho_i$ is the ice density and $L$ is the specific latent heat. This must be equal to the heat conducted through the obstacle, so that

$$\Big(k\frac{\delta T}{a}\Big)a^2 = \rho_i L u_R a^2 \quad \Rightarrow \quad u_R = \Big(\frac{kC}{\rho_i L a}\Big)\frac{\tau}{\nu^2}\,, \tag{20}$$

where $k$ is the thermal conductivity of the bedrock. It follows regelation is important for small obstacle sizes of size $a$.

Meanwhile, the velocity due to viscous shearing is related to Glen's flow law. It is

$$u_V \approx 2aA\Big(\frac{\tau}{\nu^2}\Big)^n\,, \tag{21}$$

where $n$ is the exponent in Glen's flow law. Thus, this velocity dominates for large obstacles of size $a$.

There is a controlling obstacle size $a$ for which both effects are important. Selecting $a$ so that both velocities are equal, means that $u = u_R = u_V$, so that multiplying both equations yields,

$$\tau = \nu^2\Big(\frac{\rho_i L}{2kCA}\Big)^{\frac{1}{n+1}} u^{\frac{2}{n+1}}\,. \tag{22}$$

This is known as Weertman's sliding law.

## 2.2 Lliboutry cavitation

For large obstacles, cavities are formed due to the fact that the film pressure after the obstacle is lower than the water pressure in the local subglacial drainage system. In practice, it is common to find these cavities. Figure 9 illustrates this cavitation.

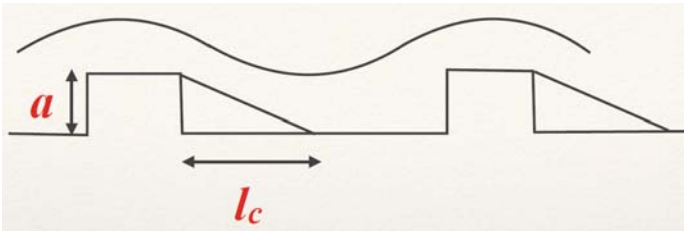


Figure 9: Lliboutry cavitation.

In this case, the velocity due to viscous shearing, which is assumed to dominate, takes the form

$$u \approx 2(a + l_c)A\Big(\frac{\tau}{\nu^2}\Big)^n\,, \tag{23}$$

where $l_c$ is the length of the cavity. Additionally, the pressure difference between the ice and water relates to the velocity by

$$\frac{u}{l_c} = AN^n\,, \qquad N = p_i - p_w\,, \tag{24}$$

where $N$ is the effective pressure, $p_i$ is the ice pressure (or overburden pressure) and $p_w$ is the water pressure. Substituting $l_c$ then yields

$$\frac{\tau}{N} = \nu^2 \Big( \frac{\Lambda}{2(1+\Lambda)} \Big)^{\frac{1}{n}}, \qquad \Lambda = \frac{u}{AN^n a}\,. \tag{25}$$

### 2.3 Drainage and the Nye-Röthlisberger model

Weertman films have a tendency to become unstable. In these cases, Röthlisberger channels form, where water flows from regions of higher pressure to regions of lower pressure. The channels are maintained open by melting in the channel walls. The melting is due to the frictional heat resulting from the flow of the water itself. The channels are schematically shown in Figure 10.

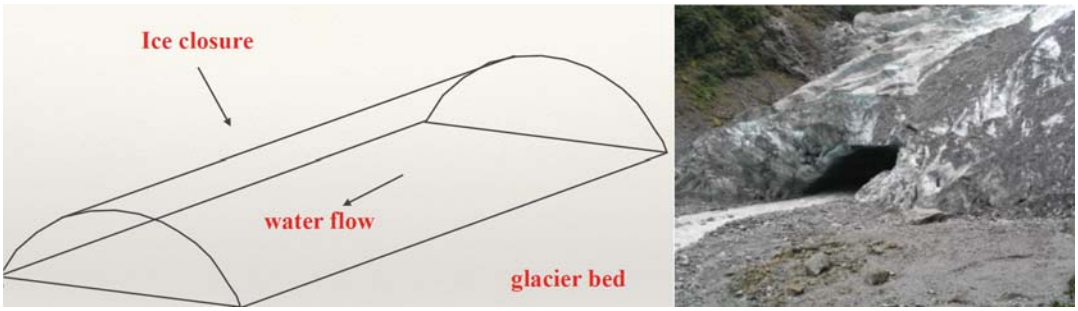


Figure 10: Röthlisberger channels.

The Nye-Röthlisberger model assumes that a channel of cross-sectional semi-circular area $S$ is governed by the closure equation

$$\frac{\partial S}{\partial t} = \underbrace{\frac{m}{\rho_i}}_{\text{melt}} - \underbrace{KSN^n}_{\substack{\text{viscous closure} \\ \text{due to ice creep}}}\,, \tag{26}$$

where $m$ is the melt rate, $K$ is a constant (proportional to $A$) derived from the ice creep problem, and $N$ is the effective pressure (see (24)).

Conservation of mass in the slowly varying channel can be written as

$$\frac{\partial S}{\partial t} + \frac{\partial Q}{\partial x} = \underbrace{\frac{m}{\rho_w}}_{\substack{\text{volume source due} \\ \text{to side-wall melt}}} + M\,, \tag{27}$$

where $x$ is the downstream spatial coordinate, $Q$ is the volume flux, $\rho_w$ is the water density, and $M$ is a prescribed source accounting for tributary flow, surface melt-water supply, etc.

Ignoring inertial terms and using a Manning correlation to account for turbulent friction, the conservation of momentum can be written as

$$\underbrace{\rho_w g \sin\alpha - \frac{\partial p_w}{\partial x}}_{\text{hydraulic gradient}} = f \rho_w g \frac{Q|Q|}{S^{8/3}}\,, \tag{28}$$

where $g$ is gravity, $f$ is a friction coefficient related to the Manning roughness factor and $\alpha$ is the mean bedrock slope.

Meanwhile, the energy equation is given by

$$\underbrace{\rho_w c_w\Big(S\frac{\partial\theta_w}{\partial t}+Q\frac{\partial\theta_w}{\partial x}\Big)}_{\substack{\text{material rate of change}\\ \text{of water temperature}}}=\underbrace{Q\Big(\rho_w g\sin\alpha-\frac{\partial p_w}{\partial x}\Big)}_{\text{frictional heat source}}-\underbrace{m\big(L+c_w(\theta_w-\theta_i)\big)}_{\substack{\text{enthalpy change}\\ \text{on melting}}}, \tag{29}$$

where $\theta_w$ is the water temperature, $\theta_i$ is the ice temperature, $c_w$ is the specific heat capacity of water, and $L$ is the specific latent heat.

Lastly, a local heat transfer condition at the ice wall for a cylindrical tube is given by

$$a_{DB}\Big(\frac{\rho_w|Q|}{\eta_w S^{1/2}}\Big)^{0.8}k(\theta_w-\theta_i)=m\big(L+c_w(\theta_w-\theta_i)\big)\,, \tag{30}$$

where $a_{DB}$ is a constant, $\eta_w$ is the viscosity of water and $k$ is the thermal conductivity of water.

The five equations, (26)–(30), constitute the Nye-Röthlisberger model which solves for the five unknowns $S$, $Q$, $m$, $p_w$ and $\theta_w$.

The effective pressure can be estimated under the assumption of steady state conditions. In this case, the equations reduce to

$$\begin{aligned}\frac{m}{\rho_i}&=KSN^n\,,\\ \rho_w g\sin\alpha-\frac{\partial p_w}{\partial x}&=f\rho_w g\frac{Q^2}{S^{8/3}}\,,\\ mL&=Q\Big(\rho_w g\sin\alpha-\frac{\partial p_w}{\partial x}\Big)\,.\end{aligned} \tag{31}$$

These equations can be solved numerically, but in general it is found that $\frac{\partial p_w}{\partial x}\ll\rho_w g\sin\alpha$, and neglecting $\frac{\partial p_w}{\partial x}$ yields a boundary layer, so that away from the snout it follows that

$$N=\Big(\frac{m}{KS\rho_i}\Big)^{\frac{1}{n}}\,,\quad S\approx\Big(\frac{fQ^2}{\sin\alpha}\Big)^{\frac{3}{8}}\,,\quad m\approx\frac{Q}{L}\rho_w g\sin\alpha\,. \tag{32}$$

Lastly, substituting the latter two in the former yields that the effective pressure is

$$N\approx\beta Q^{\frac{1}{4n}}\,,\qquad \beta=\Big(\frac{\rho_w g\sin^{11/8}\alpha}{\rho_i LKf^{3/8}}\Big)^{\frac{1}{n}}\,, \tag{33}$$

where sometimes $f$ is taken as $f=(n')^2G$, where $n'$ is the Manning roughness factor, and $G=(\frac{\ell^2}{S})^{2/3}$ is a geometric factor with $\ell$ being the wetted perimeter.

### 2.4 Linked cavities

Next, one might consider linked cavities such as those shown in Figure 11. Let $s$ be the shadowing function which represents the fraction of the bed that is cavity-free. It is a decreasing function of

$$\Lambda=\frac{u}{N^n}\,, \tag{34}$$

where $u$ is the sliding velocity. Then using the theory yields that

$$\frac{n_K^{1/4n} N}{s(\Lambda)} \approx \beta Q^{\frac{1}{4n}} , \tag{35}$$

where $n_K$ is the number of cavities across the width of the glacier. Therefore, linked cavities within a glacier operate at a higher pressure than a channel-based system.

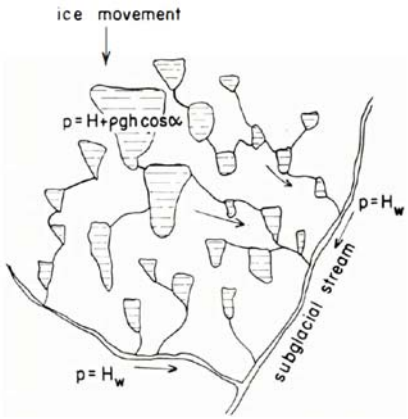


Figure 11: Linked cavities.

### 2.5 Creyts-Schoof water film

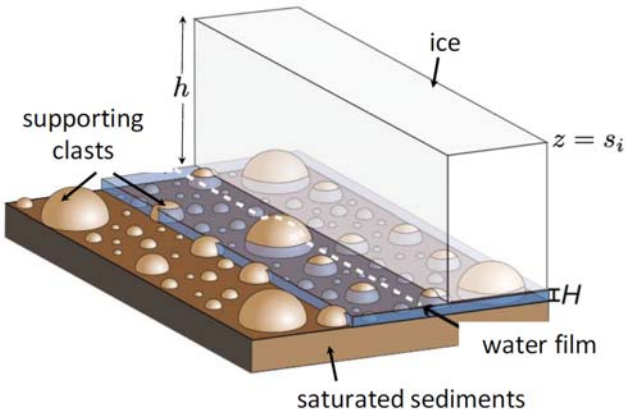


Figure 12: Creyts-Schoof water film [Creyts and Schoof, 2009].

There are other models for the films of water that develop between the bedrock and the ice. One of the most recent is the Creyts-Schoof water film [Creyts and Schoof, 2009]. Under this model, the "obstacles" actually become supporting clasts for the ice, as shown in Figure 12. In this case, there is a different scaling for the effective pressure,

$$Q \sim h^3 , \qquad N \sim \frac{1}{h^{3\mu}} , \quad \Rightarrow \quad N \sim \frac{1}{Q^{\mu}} . \tag{36}$$

## References

Creyts, T. T. and Schoof, C. G. (2009). Drainage through sub-glacial water sheets. *Journal of Geophysical Research: Earth Surface*, 114(F4).

Cuffey, K. M. and Paterson, W. S. B. (2010). *The Physics of Glaciers*. Academic Press.

Fowler, A. (2011). *Mathematical Geoscience*, volume 36. Springer Science & Business Media.

Huybrechts, P. (2007). Ice sheet modelling. In: Riffenburgh, B., editor, *Encyclopedia of the Antarctic*, pages 514–517. Taylor & Francis.